Hadronization by color bremsstrahlung

J. F. Gunion* and G. Bertsch†

Institute for Theoretical Physics, University of California, Santa Barbara, California 93106

(Received 20 July 1981)

Particle production in the central plateau of hadronic final states is calculated in a perturbative QCD model. We assume that the controlling process is bremsstrahlung of gluons. We find important differences between the spectrum produced in soft hadronic collisions and the spectrum in e^+e^- annihilation. Describing soft hadronic collisions with the Low-Nussinov model, we find that the central plateau is independent of total energy, but depends strongly on the momentum transfer in the soft-gluon exchange. In contrast, the quark jets from e^+e^- annihilation have a central plateau growing with energy. The strong momentum dependence in the hadron-induced plateau arises from the cancellations in the amplitude associated with the gauge invariance of the theory.

I. INTRODUCTION

In perturbative quantum chromodynamics (QCD) the evolution of color jets in hard interactions is a sequential process, describable by classes of Feynman diagrams as in the jet calculus.[1] For example, in e^+e^- annihilation, the particle production is initiated by perturbatively produced radiation which begins immediately after the creation of the q and $\bar{q}$ jets. Eventually the nonperturbative confinement aspects of QCD become dominant and the radiation products materialize as hadrons. Nevertheless in this description it is the underlying perturbatively produced color quanta which largely determine the distribution and multiplicity of final-state particles.

Whether or not such ideas are applicable to hadron-hadron collisions has been a subject of continuing debate. At currently available energies, the experimental multiplicities of hadron-hadron and e^+e^- final states are about the same. Theoretically, the mechanism behind this universality is not apparent. We will investigate this question in the context of the Low-Nussinov model for hadron-hadron interactions.[2] In this model the constant total cross section arises from the exchange of a gluon between quarks in the colliding hadrons, as in Fig. 1. After this gluon exchange, the state consists of two rapidly separating color octets, analogous to the separating q and $\bar{q}$ color triplets produced by e^+e^- annihilation, as in Fig. 2(a). In both cases the color separation will lead to bremsstrahlung radiation. The relationship between the final states will depend upon the relative distribu-

tion of radiation products in the two cases.

We present results here for this comparison at the simplest level—lowest-order perturbation theory with one radiated gluon. We focus on the central plateau region. In e^+e^- annihilation, the calculation is quite easy. At high energy, and in an appropriate gauge, there is only one diagram to compute, Fig. 2(b). For the case of hadron collisions, we must consider all diagrams, to a given order in the coupling constant, to arrive at a gauge-invariant result. The important diagrams
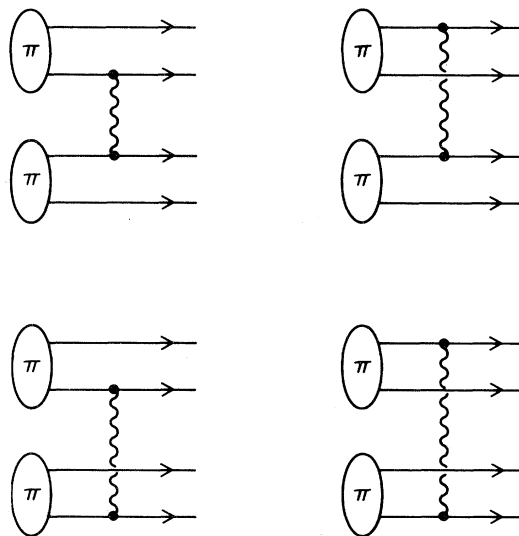

FIG. 1. Feynman diagrams for the total hadron-hadron cross section in the Low-Nussinov, gluon-exchange model.
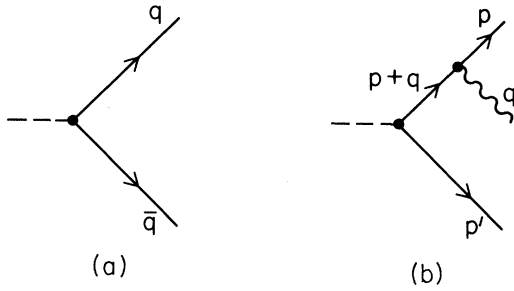
FIG. 2. (a) The Feynman diagram for virtual-photon production of a quark (q) and antiquark ($\bar{q}$) pair. (b) The Feynman diagram for gluon radiation in the quark-antiquark final state. (q labels the gluon momentum.)

will be the first three in Fig. 3. These include diagrams in which the gluon is produced from the interacting quark either prior to the soft-gluon exchange or after the soft-gluon exchange, and the diagram where the radiated gluon is emitted from the exchanged gluon. Diagrams in which the radiation comes from a spectator quark, as in Fig. 3(d), are not important in the central region. The resulting bremsstrahlung spectrum depends critically upon the interference and cancellations between the three contributions. This is to be contrasted with models which emphasize only one of these mechanisms. In the parton and multiperipheral models, the final particles are virtually present in
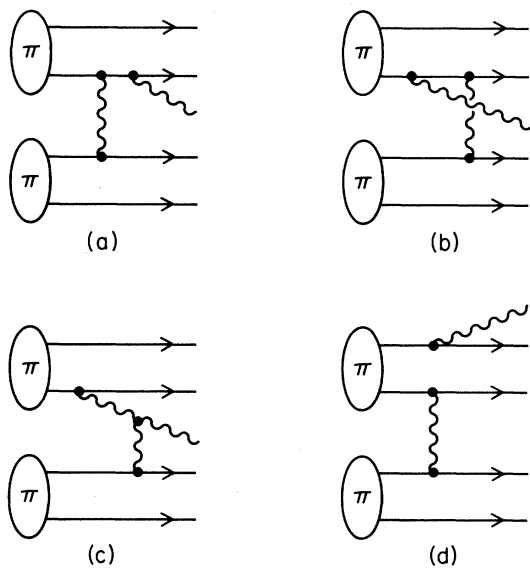

FIG. 3. Feynman diagrams for gluon radiation in hadron-hadron collisions.

the initial projectile wave function, as in Figs. 3(b) and 3(c). In the color-string picture, the color charges of the separating jets determine the final state. The perturbative calculation for this would include diagrams 3(a) and 3(d) only. In the full calculation, the strong cancellation between the amplitudes gives rise to an energy-independent density of radiation in the central region of hadron-hadron collisions; in e^+e^- annihilation there is only one diagram and no cancellation and the density rises logarithmically with s.

II. e^+e^- JETS

We begin by reviewing the theory of color bremsstrahlung for the quark jets produced in e^+e^- annihilation. We use the light-cone representation of four-vectors,

$$p = (p^+, p^-, p_\perp)$$
$$= (p_0 + p_3, p_0 - p_3, p_1, p_2) \ .$$

The variables for the radiation process are defined in Fig. 2(b). We choose the frame

$$q = (x\sqrt{s}, q_\perp^2/x\sqrt{s}, q_\perp, 0) \ ,$$

$$p = \left[(1-x)\sqrt{s}, \frac{q_\perp^2}{(1-x)\sqrt{s}}, -q_\perp, 0 \right] \ ,$$

$$p' = \left[0, \sqrt{s} - \frac{q_\perp^2}{x(1-x)\sqrt{s}}, 0, 0 \right] \ .$$

The variable x is the fractional $+-$ momentum carried by the radiated gluon relative to the maximum available, and $q_\perp$ is the transverse momentum of the gluon relative to the primordial jet direction. These variables are related to rapidity by

$$\eta = \frac{1}{2} \ln \frac{q_0 + q_3}{q_0 - q_3} = \ln \frac{x\sqrt{s}}{q_\perp} \ . \tag{1}$$

The central region is located at $\eta \sim 0$ or $x \sim q_\perp/\sqrt{s}$; radiation in the direction of the p or p' jets has $x > q_\perp/\sqrt{s}$ or $x < q_\perp/\sqrt{s}$, respectively.

We calculate the gluon field in a gauge with $A^+ = 0$. For a radiated gluon of momentum q, the allowed polarizations are

$$\epsilon_1 = (0,0,0,1) \ ,$$

$$\epsilon_2 = (0, 2q_\perp/x\sqrt{s}, 1, 0) \ . \tag{2}$$

With our gauge choice, the radiation in both jet directions arises from the same diagram, Fig. 2(b);

the diagram in which the radiated gluon is attached to the p' line is zero. The Feynman amplitude for the one-gluon emission of Fig. 2(b), divided by the amplitude for the total cross section, Fig. 2(a), is just the matrix element of the gluon field multiplied by the additional quark propagator. In the central region this is

$$\frac{\mathcal{M}_g}{\mathcal{M}_0} = \frac{\epsilon_2 \cdot (p+p-q)}{(p+q)^2} g_s \sim \frac{2q_\perp/x}{q_\perp^2/x} g_s , \tag{3}$$

where $g_s = (4\pi\alpha_s)^{1/2}$ is the QCD coupling constant. The above algebraic expression follows immediately from the Feynman rules for charged bosons, but the results in the central region are independent of quark spin. The probability of radiating a gluon near $\eta \sim 0$ is given by

$$\int dn \sim \int \frac{d^4q}{(2\pi)^4} 2\pi\delta(q^2) \left| \frac{\mathcal{M}_g}{\mathcal{M}_0} \right|^2 C_F$$

$$\sim \frac{1}{2(2\pi)^3} \int \frac{dx}{x} d^2q_\perp \frac{4g_s^2}{q_\perp^2} C_F , \tag{4}$$

where $C_F = \frac{4}{3}$ is the standard color factor for this situation. The multiplicity distribution is then given by the differential of this expression, i.e.,

$$\frac{dn_g}{dx\, d^2q_\perp} = \frac{C_F\alpha_s}{\pi^2} \frac{1}{xq_\perp^2} . \tag{5}$$

This distribution is uniform in rapidity,

$$\frac{dn_g}{d\eta\, d^2q_\perp} = \frac{C_F\alpha_s}{\pi^2} \frac{1}{q_\perp^2} . \tag{6}$$

To relate this gluon distribution to an observable quantity, assume that f_{ch} charged particles are produced in the final state for each perturbative gluon. We also integrate over $q_\perp$, with a lower limit $q_\perp \sim \Lambda$ determined by confinement, and an upper limit $q_\perp^2 \sim s$ determined by kinematics. The charged-particle distribution is then

$$\frac{dn_{ch}}{d\eta} \sim \frac{C_F f_{ch}\alpha_s}{\pi} \ln(s/\Lambda^2) . \tag{7}$$

This lowest-order perturbation result ignores possible dependence of α_s on $q_\perp$. Generalization to higher order in perturbation theory leads to a different functional form, which incorporates a moving coupling constant and higher-order emission graphs.[3] The crucial feature of Eq. (7) is that the central plateau height rises with energy as the high-$q_\perp$ tail of the gluon spectrum becomes impor-

tant. This same $1/q_\perp^2$ spectrum leads to the increase in $\langle p_T \rangle_{ch}$ observed in the e^+e^- final state, i.e., to jet broadening. The total multiplicity has an additional $\ln s$ factor from the expanding range in rapidity, $\int d\eta \sim \ln s$,

$$\langle n \rangle \cong a + b \ln s + C_F f_{ch}\alpha_s(\ln s)^2/\pi . \tag{8}$$

This form provides an excellent fit to existing multiplicity data, with the third term $\sim 0.2(\ln s)^2$ (Ref. 4). This implies that $\alpha_s \sim 0.45$, which is consistent with the strong coupling constant needed for other low-p_T phenomena.[5] We may determine the cutoff Λ in Eq. (7) by fitting the central plateau in e^+e^- annihilation jets. For example, we find $\Lambda \sim 0.2$ GeV from the empirical distribution[6] at $\sqrt{s} = 10$ GeV, $dn_{ch}/d\eta \vert_0 \sim 1.7$. This cutoff is consistent with expectations based on hadron sizes.

However, the perturbative explanation of the observed rise in $\langle n \rangle_{ch}$ and $dn_{ch}/d\eta \vert_0$ has recently been challenged.[7] Modeling the hadronization with Monte Carlo calculations[8] employing the known resonances in the Feynman-Field fragmentation functions, it is found that most of the increase in $\langle n \rangle$ can be associated with the increased phase space. Only a small contribution to $\langle n \rangle$ from the $q\bar{q}g$ high-$q_\perp$ tail is apparent. In other words, at currently available energies the multiplicity rise could be kinematic in origin. This requires further experimental study. Certainly at LEP energies a direct connection between the increase in $\langle p_T \rangle_{hadron}$ and the rise of $\langle n \rangle_{hadron}$ should be apparent.

III. RADIATION FROM QUARK SCATTERING

We now turn to hadron collisions. We assume that the underlying primary interaction is color exchange between quark constituents. The total cross section is described perturbatively by the Low-Nussinov model, shown in Fig. 1. This model successfully predicts the global features of the hadronic-collision cross sections.[2,5] These features include approximate energy independence, quark-counting rules, large diffractive cross sections,[9] and dependence of cross section on hadron size. We will calculate the gluon radiation accompanying the Low-Nussinov interaction process. It is convenient to first consider the collision of two quarks. Later we will assemble the quarks into color-neutral hadrons. The lowest-order contributions to the amplitude come from the diagrams of Fig. 4. The four-vectors defined in Fig. 4 are
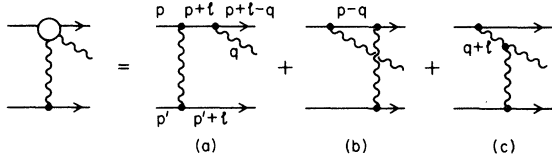
FIG. 4. Feynman diagrams for the lowest-order contributions to gluon radiation in quark scattering. Diagrams not shown do not contribute in the $x \rightarrow 0$ limit for our gauge choice.

$$p = (\sqrt{s}, 0, 0, 0) ,$$

$$p' = (0, \sqrt{s}, 0, 0) ,$$

$$q = (x\sqrt{s}, q_\perp^2/x\sqrt{s}, q_\perp, 0) , \qquad (9)$$

$$l = (l^+, l^-, l_\perp) .$$

The conditions that the quarks be on shell, $(p'-l)^2 = 0$ and $(p+l-q)^2 = 0$, imply

$$l_+ \cong -l_\perp^2/\sqrt{s} , \qquad (10)$$

$$l_- \cong \frac{q_\perp^2/x + l_\perp^2 - 2q_\perp \cdot l_\perp}{(1-x)\sqrt{s}} .$$

With these kinematics the computation of Figs. 4(a)−4(c) is straight forward. We consider only terms in the amplitude which are proportional to s. The amplitudes will be expressed in terms of the elastic scattering amplitude,

$$\mathcal{M}_{g^2} = \frac{2sg_s^2}{l_\perp^2} \times (\text{color matrix element}) \qquad (11)$$

which is obtained in the absence of radiation. This amplitude contains an infrared divergence, $1/l_\perp^2$, which will be regulated once the quarks are placed in hadrons. For a given polarization, the amplitudes of Figs. 4(a)−4(c) are, respectively,

$$\frac{\mathcal{M}_{g^3}}{\mathcal{M}_{g^2}} = \begin{cases} 2g_s \dfrac{(\vec{q}_\perp - x\vec{l}_\perp)\cdot\vec{\epsilon}_\perp(1-x)}{(x\vec{l}_\perp - \vec{q}_\perp)^2} C_{(a)} & (12a) \\[4mm] -2g_s \dfrac{\vec{q}_\perp\cdot\vec{\epsilon}_\perp(1-x)}{q_\perp^2} C_{(b)} & (12b) \\[4mm] 2g_s \dfrac{(\vec{l}_\perp - \vec{q}_\perp)\cdot\vec{\epsilon}_\perp(1-x)}{(\vec{q}_\perp - \vec{l}_\perp)^2} C_{(c)} & (12c) \end{cases}$$

The factors $C_{(a)}$, $C_{(b)}$, and $C_{(c)}$ are the color-algebra matrix elements associated with the diagrams 4(a)−4(c), divided by the color factor present in the absence of radiation. In an Abelian case such as electrodynamics, the two nonvanishing diagrams (a) and (b) cancel if $xl_\perp$ is not comparable to $q_\perp$. For a fixed finite $l_\perp$, the order of magnitude

of the photon's rapidity is then

$$\eta = \ln\frac{x\sqrt{s}}{q_\perp} \sim \ln\frac{\sqrt{s}}{l_\perp} . \qquad (13)$$

Thus the radiation is confined to a region within

$$\Delta\eta = \left|\ln\frac{\sqrt{s}}{l_\perp} - \ln\frac{\sqrt{s}}{m}\right| = \left|\ln\frac{m}{l_\perp}\right| \qquad (14)$$

of the projectile rapidity. A similar radiation pattern in the target fragmentation region is obtained by considering the diagrams analogous to Fig. 4 in which the photon attaches to the p' legs of the scattering diagram. At any finite rapidity value in the central region, the radiation falls as a power of s. Intuitively these results are obvious. The amount of charge acceleration in the Abelian theory is controlled by $l_\perp$, since the charge of the particle does not change. Thus the radiation is limited to the rapidity interval over which the charge is accelerated.

The non-Abelian QCD results are completely different. The exchanged gluon carries color so that the quark colors can change. Thus charge acceleration can take place over the full rapidity interval between projectile and target, even if $\langle l_\perp^2 \rangle$ is finite. To study the central plateau, the sum of amplitudes (12a)−(12c) is evaluated in the limit $xl_\perp \ll q_\perp$. We will call this limit the "$x \rightarrow 0$" region. It includes the $\eta \sim 0$, $x \sim q_\perp/\sqrt{s}$ central region. The sum of (12a)−(12c) then reduces to

$$|\mathcal{M}_{g^3}/\mathcal{M}_{g^2}|^2 \cong C_{(c)}^2 4g_s^2 \frac{l_\perp^2}{q_\perp^2(q_\perp - l_\perp)^2} . \qquad (15)$$

This corresponds to a multiplicity distribution at fixed $l_\perp$ of

$$\frac{dn_g}{d\eta\, d^2q_\perp} \cong \frac{C_{(c)}^2 \alpha_s}{\pi^2} \frac{l_\perp^2}{q_\perp^2(q_\perp - l_\perp)^2} . \qquad (16)$$

From this form it is clear that there is a uniformly populated central plateau, with a *limited* $q_\perp$ spectrum. While at small $q_\perp < l_\perp$ the result is similar to the e^+e^- result, at large $q_\perp$ the spectrum falls as $1/q_\perp^4$, leading to a finite $\langle q_\perp^2 \rangle$. There is no growth in the plateau height with s due to a high-$q_\perp$ tail. Another interesting point is that the cancellation between (12a)−(12c) is complete for $l_\perp = 0$ in the central region. Gauge invariance requires that the scattering process change more than the color labels at the vertices, for radiation to be produced. We will remark further on these results after combining the quark amplitudes for a model of hadron interactions.
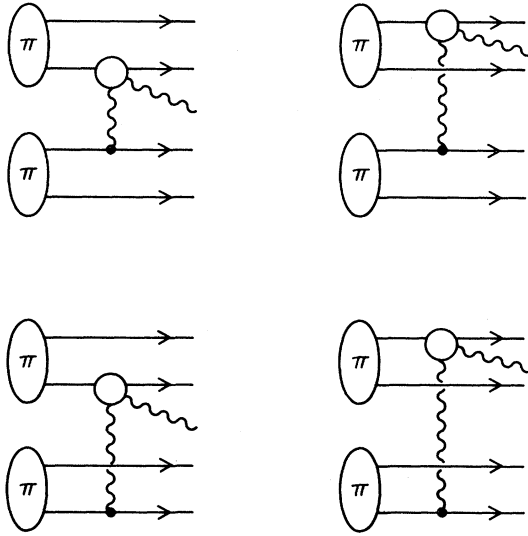
FIG. 5. Feynman diagrams for $x \to 0$ radiation in the Low-Nussinov model of hadron-hadron scattering. The circle vertex includes the three diagrams appearing in Fig. 4.

FIG. 6. A Feynman diagram for gluon radiation which does not contribute in the $x \to 0$ limit because the Low-Nussinov-exchange gluon is not contiguous to the radiated gluon.

IV. HADRON MULTIPLICITY DISTRIBUTIONS

First it is necessary to recall the form of the Low-Nussinov cross section in the absence of radiation. We consider π-π collisions for simplicity.[5] The four diagrams in Fig. 1 are summed and squared to give a cross section

$$\sigma_{\pi\pi} = \alpha_s^2 \int \frac{d^2 l_\perp}{l_\perp^4} (2)[1 - f_{q\bar{q}}^{\mathrm{I}}(l_\perp^2)]$$

$$\times (2)[1 - f_{q\bar{q}}^{\mathrm{II}}(l_\perp^2)] . \tag{17}$$

Here the (2)'s are the quark-counting factors. The $f_{q\bar{q}}(l_\perp^2)$ is a form factor which satisfies $f_{q\bar{q}}(0) = 1$, and is approximately equal to the usual meson form factor $F(Q^2 = 4l_\perp^2)$. Note that the $1/l_\perp^4$ infrared divergence of the gluon exchange is now regulated by the vanishing of the $1 - f_{q\bar{q}}(l_\perp^2)$ factors as $l_\perp^2 \to 0$. The relative minus signs in Eq. (17) arise from the interference between diagrams where the gluon attaches the quark and antiquark of the

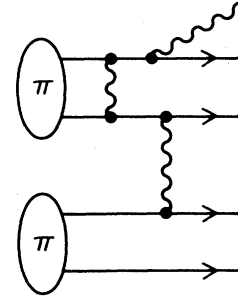color-singlet meson. The interference amplitudes have initial and final hadron wave functions evaluated at momenta differing by $l_\perp$, giving rise to the form factors $f_{q\bar{q}}(l_\perp^2)$.

Now let us calculate the radiation diagrams which occur in the Low-Nussinov model. Figure 5 shows the diagrams which are dominant in the previously defined $x \to 0$ limit. Note that the radiation must occur contiguous to the exchanged Low-Nussinov gluon. In particular, radiation from spectator quarks in the hadron wave function is suppressed. This comes about because any diagram such as Fig. 6 connecting the radiated gluon to the Low-Nussinov exchange gluon contains extra intermediate lines which are off shell by an amount of order $q_\perp^2/x$. In the "$x \to 0$" limit, especially in the central region, these propagators give extra factors of x in the amplitude. Consequently such diagrams contribute at large s to the projectile fragmentation region and not to the central plateau.

The amplitudes of Fig. 5 interfere destructively as in the Low-Nussinov cross section. The effective color factor $C_{(a)}^2$ is computed in Cvitanovic's diagrammatic approach[10] as

The resulting gluon radiation cross section from Figs. 5 is given by the following in the "$x = 0$" limit:

$$\frac{d\sigma}{dx \, d^2 q_\perp} \cong \frac{C_A \alpha_s^3}{\pi^2 x q_\perp^2} \int \frac{d^2 l_\perp}{l_\perp^4} \frac{l_\perp^2}{(l_\perp - q_\perp)^2} (2)[1 - f_{q\bar{q}}^{\mathrm{I}}((q_\perp - l_\perp)^2)](2)[1 - f_{q\bar{q}}^{\mathrm{II}}(l_\perp^2)] . \tag{18}$$

The interference between the different diagrams of Fig. 5 gives rise to the form factors $f_{q\bar{q}}$. The quark-radiation result, Eq. (15), appears as a multiplicative factor in Eq. (18). Note that the $l_\perp \to 0$ divergence of the quark amplitude is regulated within the color-singlet hadrons, as in the Low-Nussinov cross section.

The multiplicity of gluon radiation in the "$x \to 0$" domain is just the ratio of Eqs. (18) and (17). The ratio simplifies in two limits, depending on the size of $q_\perp^2$ compared to $\langle l_\perp^2 \rangle$. The $\langle l_\perp^2 \rangle$ is determined mainly by the hadronic wave-function form factors. If $q_\perp^2 < \langle l_\perp^2 \rangle$, the distribution looks similar to the e^+e^- annihilation result,

$$\frac{dn}{dx\,d^2q_\perp} \cong \frac{C_A \alpha_s}{\pi^2 x q_\perp^2} .$$ (19)

The only difference is that the color factor is that associated with the total charge of the octet jet, and is thus $C_A/C_F = \frac{9}{4}$ larger than that obtained in e^+e^- annihilation. This relation was suggested in Ref. (11).

At large $q_\perp$ the hadronic result is quite different from that for e^+e^- radiation. To illustrate the high-$q_\perp$ behavior of the hadronic radiation, we model the form factors with ρ dominance,

$$f_{q\bar{q}}(l_\perp^2) \sim (1 + 4l_\perp^2/m_\rho^2)^{-1} .$$ (20)

The radiation distribution is then

$$\frac{dn}{dx\,d^2q_\perp} = \frac{C_A \alpha_s}{\pi^2 x q_\perp^2} \int \frac{d^2l_\perp [(m_\rho^2 + 4l_\perp^2)(m_\rho^2 + 4(l_\perp - q_\perp)^2)]^{-1}}{\int d^2l_\perp (m_\rho^2 + 4l_\perp^2)^{-2}} .$$ (21)

This behaves asymptotically at large $q_\perp^2$ as

$$\frac{dn}{dx\,d^2q_\perp} \sim \frac{C_A \alpha_s}{\pi^2 x (q_\perp^2)^2} m_\rho^2 \ln q_\perp^2/m_\rho^2 .$$ (22)

Let us integrate over $q_\perp^2$ from Λ^2 to s, as we did for e^+e^- annihilation. Instead of the logarithmically rising central plateau we find one regulated by the ρ mass. Roughly,

$$\frac{dn^{\text{hadron}}/dx}{dn^{e^+e^-}/dx}\bigg|_{x=0} \sim \frac{C_A}{C_F} \frac{\ln m_\rho^2/\Lambda^2}{\ln s/\Lambda^2} .$$ (23)

Taking $\Lambda \cong 0.2$ GeV from our fit to the absolute e^+e^- plateau height we obtain a ratio of 0.6 at $\sqrt{s} = 30$ GeV. If the perturbative calculation is valid, this ratio should continue to decrease as s increases. The plateaus should have roughly equal heights at lower energies, roughly $\sqrt{s} \sim 4$ GeV.

In determining the α_s and Λ values from e^+e^- annihilation we assumed that the entire rise of the plateau height was perturbative in origin. The corresponding prediction in p-p collisions is, as we have seen, a roughly constant plateau height. Experimentally, there is at least a slow rise of plateau height with s, seen for example in the data of Thomé et al.[12] In their data, the plateau height falls well below the e^+e^- plateau height at the same energy, and is consistent with the final-state phase playing a minor role in determining the multiplicity. However, other data and analyses[13] suggest that the Thomé results may be incorrect and that the pp and e^+e^- plateau heights may be the same at similar energies. This would be natural if the e^+e^- and pp plateau-height rises were predominantly kinematic in origin, as suggested in Ref. 7.

Only the data of Thomé et al. is consistent with a large perturbative component to the final-particle multiplicity.

There are a number of other significant phenomenological features of our gluon-radiation calculation which are of interest. If the collisions are studied event by event, the value of $l_\perp$ will vary. Since both forward and backward hemisphere radiation is controlled by $l_\perp$, it would appear that there would be a correlation between radiation in the two hemispheres. However, a precise calculation of this correlation would require the study of amplitudes with two external gluons. Even without an $l_\perp$ dependence, these amplitudes show larger fluctuations in the multiplicity distributions than would result from Poisson statistics.[1]

Another interesting phenomenological point follows from the fact that our perturbative calculation predicts a plateau height in hadron collisions which is controlled by $\langle l_\perp^2 \rangle$. The value of $\langle l_\perp^2 \rangle$ depends on the hadron form factors, which in turn are sensitive to the size of the hadrons. Models of the hadron wave functions other than the bag model tend to have an inverse relation between the masses of the quarks in the hadron and the hadron size. For example, the sequence ρ, ϕ, ψ, Υ, should correspond to sharply decreasing hadron sizes. This implies decreasing total cross sections in the Low-Nussinov model,[5] in agreement with experiment. Here we note that $\langle l_\perp^2 \rangle$ will increase with decreasing hadron size, and thus lead to higher multiplicities in the central plateau. Unfortunately ϕ, ψ, and Υ beams are not available. The difference in size between a kaon and a pion is probably too small to prevent our effect from being over-

whelmed by the smaller available kinetic energy in the final state, due to the presence of a strange quark in the final state.

Our calculation also has a number of noteworthy theoretical features. First it is useful to relate our results to the discussion of hadron multiplicities given by Pokorski and Wolfram.[14] These authors study the hadron jets made from one-"gluon" exchange, as in Fig. 7. They find that the multiplicity growth is the same as in e^+e^- annihilation if l, the momentum transfer of the exchanged gluon, has a nonvanishing longitudinal component. Our calculation relates l_+ and l_- to $l_\perp$, $q_\perp$, x, and $\sqrt{s}$ (see Eq. 10), predicting a definite distribution for the longitudinal component. We find that the longitudinal component is small in the high-s limit, and thus multiplicities do not grow rapidly. From Fig. 7, it is also possible, using gauge invariance, to understand in a general way the sensitivity to $l_\perp$. First consider the extreme $l_\perp = 0$. Equation (10) implies that $l_+ = 0$, and thus the exchanged gluon is nearly on shell. Next we cut across the gluon in Fig. 7 and divide the amplitude into an upper component T_α and lower component T'_α. These partial amplitudes obey the gauge invariance conditions $l_\alpha T'_\alpha = l_\alpha T_\alpha = 0$ at $l^2 = 0$, since the other external legs are presumed to be physical on-shell states. This in turn implies $T_- = 0$ and $T'_- = 0$. Now combine the partial amplitudes for a total

$$A \cong -T_\alpha T'_\beta g_{\alpha\beta} = T_\perp \cdot T'_\perp .\qquad (24)$$

Both $T_\perp$ and $T'_\perp$ are of order 1, considered as a function of s, and thus the amplitude A is finite at high s. But to make a cross section finite at large s the amplitude must be proportional to s; this can only be done with the T_+ and T'_- components that are present when $l \neq 0$.

As a second major point, we wish to reemphasize the crucial importance of interference effects in our calculation. These occur both at the level of individual quarks radiating gluons, and at
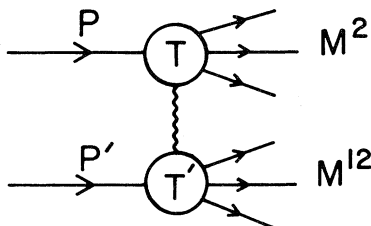
the level of the hadrons composed of quarks in color singlets. The cancellations due to the color-singlet structure of the hadrons are crucial in regulating the $1/l_\perp^4$ singularity of the quark amplitude. This is in sharp constrast to the dual topological approach,[15] in which there are two noninterfering multiplicity chains. The interference at the quark level of diagrams 4(a)—4(c) also emphasizes the importance in a gauge-invariant calculation of including at the same time both diagrams in which the radiated gluon is emitted before and after the hadron-hadron interaction. As mentioned in the Introduction, other conventional approaches consider only one or the other possibility.

An interesting subtlety of this calculation is the notion of contiguity of the gluon spanning the large rapidity gap to the radiated gluon. The central plateau is populated only by diagrams in which the radiated gluon and the Low-Nussinov exchange gluon participate in a Compton-like subprocess. A diagram such as Fig. 8(a) survives as "$x \rightarrow 0$" whereas Fig. 8(b) and Fig. 6 are suppressed as "$x \rightarrow 0$."

Finally we note that our conclusions are unaltered if the initial-hadron Fock state contains hard intrinsic gluons, i.e., ones with no $1/x$ behavior. Soft virtual gluons in the initial-hadron wave function can become real and on-shell only through the types of perturbative diagrams considered previously; whereas a hard intrinsic gluon can be approximately on-shell without perturbative interaction and could itself radiate a soft gluon. Thus with hard intrinsic gluons, there is a new basic process of gluon-gluon Compton scattering. The diagrams of Fig. 9 contribute to the central plateau in the same way as the analogous quark amplitudes, and exhibit the same cancellations. The gauge invariance, of course, demands that the quartic gluon
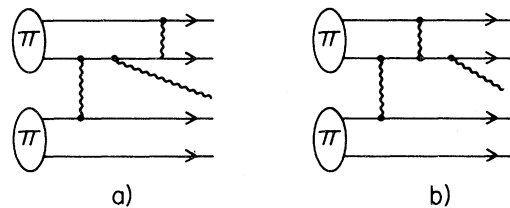

FIG. 7. Generalized Feynman diagram for the collision of two hadrons via "gluon" exchange as considered by Pokorski and Wolfram (Ref. 14).

a)   b)

FIG. 8. Typical graphs for hadron collision with gluon radiation that are higher order in α_s. In diagram (a) the radiated gluon and Low-Nussinov exchange gluon are contiguous, and therefore it survives in the $x \rightarrow 0$ limit. In diagram (b) a wave-function interaction separates the Low-Nussinov gluon for the radiated gluon, and hence this diagram is suppressed in the $x \rightarrow 0$ limit.
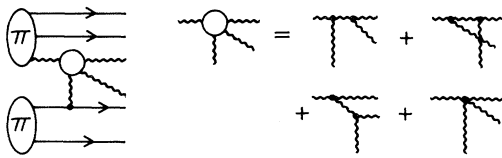
FIG. 9. Diagrams for a Low-Nussinov collision with soft-gluon radiation from a hard intrinsic Fock-state gluon. As in the quark case only the contiguous diagrams shown survive in the $x \to 0$ limit.

coupling be included to produce the required cancellation in the gluon-gluon amplitude.

In conclusion we recall that color-exchange models provide a simple and attractive explanation of the Pomeron behavior of total cross sections. Since these models imply that color separation and acceleration take place in the final state, it is of interest to investigate in that context the relationship between e^+e^- final states and hadronic-collision final states using the framework of the jet calculus. We have reported here on the first stage of this comparison—one-gluon-emission multiplicities—and found important differences in the perturbative contribution to final-state particle production. These arise directly from gauge invariance and off-shell effects intrinsic to the QCD perturbative calculations.

ACKNOWLEDGMENT

*Permanent address: Physics Department, University of California, Davis, CA 95616.

†Permanent address: Physics Department, Michigan State University, East Lansing, MI 48824.

[1] For a recent review, see K. Konishi, in Proceedings of the XI International Symposium on Multiparticle Dynamics, Bruges, 1980 (unpublished).

[2] F. E. Low, Phys. Rev. D **12**, 163 (1975); S. Nussinov, ibid. **14**, 246 (1976).

[3] W. Furmanski, R. Petronzio, and S. Pokorski, Nucl. Phys. **B155**, 253 (1979); A. Bassetto, M. Ciafaloni, and G. Marchesini, ibid. **B163**, 477 (1980).

[4] J. F. Gunion, in Proceedings of the XI International Symposium on Multiparticle Dynamics, Bruges, 1980 (unpublished); and in Proceedings of the 1981 Erice School on Low-p_T Soft Hadronic Interactions (unpublished).

[5] J. F. Gunion and D. E. Soper, Phys. Rev. D **15**, 2617 (1977).

[6] TASSO Collaboration, R. Brandelik et al., Phys. Lett. **89B**, 418 (1980).

[7] G. Wolf, in Proceedings of the XI International Symposium on Multiparticle Dynamics, Bruges, 1980 (unpublished).

[8] A. Aki, E. Pietarinen, G. Kramer, J. Willrodt, Phys. Lett. **93B**, 155 (1980); A. Ali, E. Pietarinen, and J. Willrodt, Report No. DESY-T-80-D1, 1980 (unpublished).

[9] J. Pumplin and E. Lehman, Z. Phys. C **9**, 25 (1981).

[10] P. Cvitanovic, Phys. Rev. C **14**, 1536 (1976).

[11] S. J. Brodsky and J. F. Gunion, Phys. Rev. Lett. **37**, 402 (1976).

[12] W. Thome et al., Nucl. Phys. **B129**, 365 (1977).

[13] M. Basile et al., Phys. Lett. **92B**, 367 (1980).

[14] S. Pokorski and S. Wolfram, Caltech. Report No. CALT-68-795 (unpublished).

[15] A. Capella, U. Sukhatme, and J. Tran Thanh Van, Z. Phys. C **3**, 329 (1980); G. Cohen-Tannoudji, A. El Hassouni, J. Kalinowski, O. Npaoly, and R. Peschanski, Phys. Rev. D **21**, 2699 (1980); H. Minakata, ibid. **20**, 1656 (1979).